FDP-51 / ISS2006

Submitted 6 March 2007

Terahertz electromagnetic-wave detector using Nb-based superconducting tunnel junction on $LiNbO_3$ substrate absorber

T. Taino[a, *], H. Ishii[a], S. Yoshimura[a], C. Otani[b], S. Ariyoshi[b], H. Myoren[a], K. Kawase[b], T. Shibuya[b], H. Sato[b], H. M. Shimizu[b], S. Takada[a]

Address
[a] Saitama University, 255 Shimo-Ohkubo, Sakura, Saitama 338-8570, Japan
[b] RIKEN, 2-1 Hirosawa, Wako, Saitama 351-0198, Japan

Abstract

We have been developing terahertz (THz) wave detectors using superconducting tunnel junctions (STJs). The STJs consist of the Nb/Al/AlO_x/Al/Nb structure. We fabricated THz-wave detectors on $LiNbO_3$ substrates, that have a high absorption coefficient for the frequency range of 10^{12} Hz. Two kinds of signals were detected when the THz-wave was irradiated from the substrate side. One was an indirect signal related to the generation of phonons. The other was a signal that corresponds to directly generated quasi-particles in the Nb electrode of the STJ. The pulse height of the indirect signal was larger than that of the latter signal. To enlarge the detector area, we designed a STJ that has different areas of the base electrode and top electrode. In this paper, the characteristics of the THz-wave detector area will be discussed.

PACS codes
85. 25. –j, 85. 25. Cp

keywords
Terahertz (THz) wave detector, Superconducting tunnel junction (STJ), $LiNbO_3$

* Corresponding author.
Dr. Tohru Taino
Postal address: Department of Electrical and Electronic System, Saitama University, 225 Shimo-Ohkubo, Sakura, Saitama 338-8570, Japan
Phone: +81-48-858-3899
Fax: +81-48-858-3473
E-mail address: taino@super.ees.saitama-u.ac.jp

1. Introduction

Detector performances are linked to the experimental precision of various fields such as engineering and science. Superconducting tunnel junctions (STJs) are promising candidates for next generation photon detectors, because the STJ has many favorable features, such as high-energy resolution, wide operating region and high counting rate [1-3]. For example, a theoretical energy resolution is estimated to be a few eV for photons of 6 keV.

In recent years, terahertz (THz) electromagnetic waves have become attractive for use in various research fields because this range of wavelength has photonic and electronic features [4-6]. In particular, the THz-wave are suitable for imaging applications. The progress of THz-wave studies corresponds with the development of THz-wave generator. On the other hand, the development of THz-wave detectors has not advanced compared with the development of THz-wave generator. We have proposed and demonstrated a new THz detector using the STJ [7, 8]. The STJ utilizes a $LiNbO_3$ substrate as a THz-wave absorber. The THz-wave are irradiated from the substrate side, and generate THz phonons in the substrate. Then, the propagated phonons reach the base electrode of the STJ, and break Cooper pairs in the electrode. In this method, the STJ can be operated above the subgap of the Nb superconductor (0.7 THz). This STJ detector detected waves of 1-2 THz.

To enlarge the detector area, we designed a STJ that has different areas of the base and top electrodes. In this paper, we report and discuss the detected signal of the THz-wave using the STJ with differing electrode areas.

2. STJ for THz wave detector

A typical STJ photon detector consists of a Nb/Al/AlO_x/Al/Nb structure on a substrate. Fig. 1 shows a schematic cross section of the STJ. When the photon is irradiated into the electrode of the STJ from the STJ side, the photons, which have energy greater than 2Δ, generate a great number of quasi-particles and phonons. The Δ is the energy gap in the superconductor. In Nb, since Δ is 1.5 meV, the lower limit of the operating frequency of STJ is 0.7 THz. Our proposed STJ is fabricated on a $LiNbO_3$ substrate, which is a THz-wave absorber. In addition, the THz-wave are illuminated from the substrate side. Therefore, the detector is sensitive to any type of radiation or energy input above the energy gap if the energy is supplied the substrate. Here, $LiNbO_3$ has a high absorption efficiency for waves in the THz region.

The multilayer of Nb/Al/AlO_x/Al/Nb is deposited on a $LiNbO_3$ substrate by dc-magnetron sputtering. The oxidization condition of the tunneling barrier was at 1330 Pa for 1 hour. Under this condition, the critical current density J_c was estimated to be 150 A/cm^2. The structure of the STJ was patterned by photolithography and reactive ion etching (RIE). The contact hole of 5 μm × 5 μm was formed after the deposition of SiO_2 insulator. Finally, the Nb wire of 10 μm width was deposited and formed by the RIE. Table 1 shows the film thickness of the fabricated STJ.

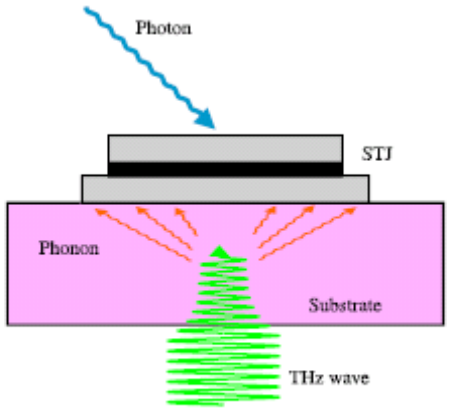

Fig. 1. Cross-sectional view of typical STJ photon detector.

To achieve a high efficiency of THz-wave detection, it is essential for the base electrode of the STJ to cover a wide area. On the other hand, the greater the area, the capacitance of the STJ becomes greater. Then, the pulse height is low. Therefore, the optimization of the areas of both top and bottom electrodes of the STJ is required. To enlarge the detector area, we designed STJs that have different areas of the base and top electrodes. Type A refers to STJ that consists of top electrode with a fixed area of 50 μm × 50 μm and a base electrode of various areas (70 μm × 70 μm, 100 μm × 100 μm, 200 μm × 200 μm, 400 μm × 400 μm, 800 μm × 800 μm). Type B refers to STJs that consist of the fixed base electrode area of 70 μm × 70 μm and different

Table 1
Specifications of fabricated STJ

Structure	Nb/Al/AlO_x/Al/Nb
Nb: wire	600 nm
SiO_2: insulator	350 nm
Nb: top electrode	150 nm
Al: trapping layer	60 nm
Nb: base electrode	200 nm
Substrate: $LiNbO_3$	500 μm
Contact hole size	5 μm × 5 μm

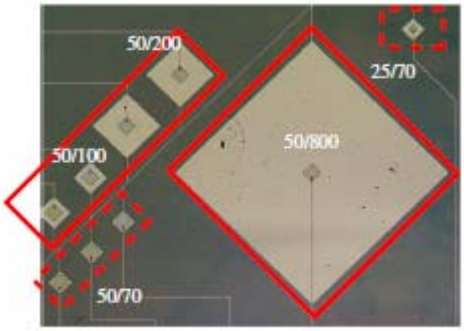

Fig. 2. The fabricated STJ.

area of top electrode (25 μm × 25 μm, 50 μm × 50 μm). All these STJs were diamond shaped. Fig. 2 shows a micrograph of the fabricated STJs in part of a chip of 5 mm × 5 mm. In this figure, the STJs designated by solid lines are type A, and the STJs designated by dashed lines are type B. The name of each STJ indicates the areas of the top and bottom electrodes. For example, the STJ with the top electrode of 50 μm × 50 μm and the base electrode of 70 μm × 70 μm was named 50 / 70.

3. Characteristics of fabricated STJ

To check the quality of fabricated the STJ, the current-voltage characteristics were measured at temperatures of 0.4 K, 1.6 K, and 4.2 K. Fig. 3 shows the temperature dependence of the subgap current at 500 μV. The vertical axis indicates the subgap current normalized by that measured at

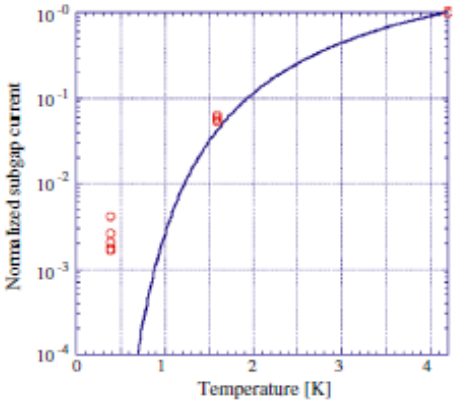

Fig. 3. Temperature dependence of the subgap current.

4.2 K. The solid line shows the calculation based on BCS theory. The circles show the measured values for the STJ. From this figure, we confirmed that the normalized current at 1.6 K was close to the values expected on the basis of the BCS theory. At 0.4 K, however, excess current in the BCS prediction was observed. This is mainly due to the additional leakage current through or at the edge of the tunnel barrier. We previously succeeded in fabricating similar junctions with lower normalized current (around 10^{-5}), but we must improve the reproducibility of our fabrication process. In this study, however, our aim is to test the STJs with different areas of the base and top electrodes in order to enlarge the detection area of THz radiation, and to use the fabricated junctions can be used to obtain the required data for optimizing the detector design.

4. THz-wave detection experiment

To investigate the most suitable area of the STJ to be used as a THz-wave detector, we designed STJs with different areas of the base and top electrodes. For the THz-wave detection experiment, the fabricated STJs on $LiNbO_3$ substrate absorbers were placed on a Si hyperhemispherical lens in a ^{3}He cryostat. The STJs were refrigerated to 0.4 K. To suppress dc Josephson current, a superconducting coil was used to apply a magnetic field of about 5 mT. When the THz-wave was illuminated on to the STJ, the excess current was fed to a preamplifier at room temperature. The waveforms of detected signals were monitored on an oscilloscope. THz pulses with a reputation frequency of 49 Hz were generated using a terahertz parametric oscillator (TPO) [9, 10].

First, we investigated whether the pulse height depends on the area of the base electrode. We compared the pulse heights using type A STJs, as shown in Fig. 4. The horizontal axis indicates the area of base electrodes. The frequency of the input THz pulse was 1.4 THz. Each pulse height in this figure is the average of 300 observed pulse height data. In this figure, the pulse height is seen to decrease slightly with the area of the base electrodes. However this tendency seems to be almost constant when taking into account the distance between the center of the THz spot and STJs, because the spot

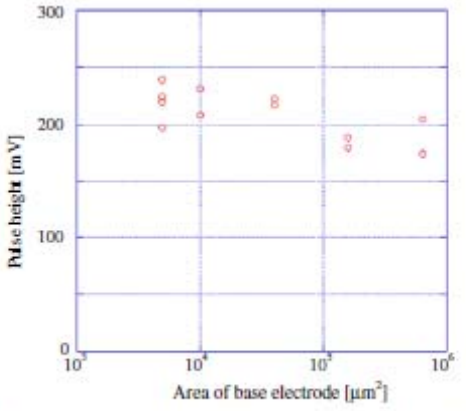

Fig. 4. Dependence of pulse height on area of base electrode.

size of THz-wave was estimated to be about 1 mm in diameter. In this experiment, all measured STJ were not illuminated by the THz beam. Therefore, we concluded that the pulse heights do not depend on the area of base electrodes.

Next, we investigated be the pulse height depends on the area of the top electrode. We compared the pulse height using type B STJs, as shown in Fig. 5. The horizontal axis indicates the area of top electrodes. The area of top electrodes is

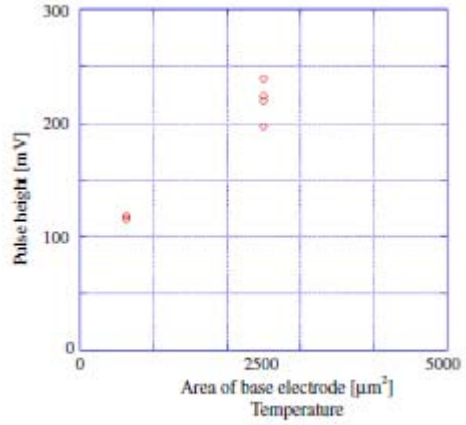

Fig. 5. Dependence of pulse height on area of top electrode.

equal to the tunnel junction area. The pulse heights increased with increasing junction area, but were not proportional to the junction area. This implied that the area just outside of the junction area also contributed to the pulse heights. Quasi-particles generated by phonons from the $LiNbO_3$ substrate absorber can diffuse within the diffusion length of about 10 μm in the bottom electrodes and can contribute to tunnel current and pulse height.

Referring to the above results, we can design STJs for THz-wave detection that take into account the quasi-particle diffusion length λ in the bottom electrodes. For instance, assuming the length of a junction to be x, the pulse height should be proportional to $(x + 2\lambda)^2$. The diffusion length estimated from the experimental results, shown in Fig. 5 was 7 μm. A theoretical λ of about 10 mm was calculated [11]. To verify this equation, further experiments are planned, including those on designing a new photomask and on THz-wave irradiation of the newly designed STJs.

5. Conclusion

To enlarge the area of THz-wave detectors, we designed and fabricated STJs with different areas of the base electrodes and top electrodes. The fabricated STJs showed relatively good current-voltage characteristics that almost correspond to the BCS theory. The STJ were cooled to the operating temperature of 0.4 K using a ^{3}He cryostat. We observed the waveform for THz-wave pulse irradiation from various STJs, which enabled us to design the STJs for THz-wave detection, taking into account the quasi-particle diffusion length λ in the bottom electrodes.

Acknowledgement

We would like to thank Dr. M. Kurakado of RIKEN for valuable discussions. This work was supported by Grant-in-Aid 18686009 from the Ministry of Education, Culture, Sports, Science and Technology of the Japanese Government, and also partially supported by grants from Saitama University.

References

[1] M. Frank, L. J. Hiller, J. B. Grand, C. A. Mears, S. E. Labov, M. A. Lindeman, H. Netel, D. Chow, A. T. Barfknech, Rev. Sci. Instrum. 69 (1998) 25.
[2] G. Angloher, P. Hettl, M. Huber, J. Jochum, F. v. Feilitzsch, R. L. M□βbauer, J. Appl. Phys. 89 (2001) 1425.
[3] M. Frank, C. A. Mears, S. E. Labov, F. A. Lindemam, L. J. Hiller, H. Netel, A. Barknecth, Nucl. Instrum. Methods. A370 (1996) 41.
[4] B. B. Hu, M. C. Nuss, Opt. Lett. 20 (1995) 1716.
[5] M. Yamashita, T. Kiwa, M. Tonouchi, K. Nikawa, C. Otani, K. Kawase, IRMMW/THz2004, Germany, Th3.2.
[6] K. Kawase, Y. Ogawa, Y. Watanabe, Opt. Exp. 11 (2003) 2549.
[7] C. Otani, T. Taino, R. Nakano, K. Hoshino, T. Shibuya, H. Myoren, S. Ariyoshi, H. Sato, H. M. Shimizu, S. Takada, K. Kawase, IEEE. Trans. Appl. Supercond. 15 (2005) 591.
[8] T. Taino, R. Nakano, S. Yoshimura, H. Myoren, S. Takada, C. Otani, S. Ariyoshi, T. Shibuya, K. Kawase, H. Sato, H. M. Shimizu, Nucl. Instr. Methods. Phys. Res. A 559 (2006) 751.
[9] K. Kawase, J. Shikata, H. Ito, J. Phys. D: Appl. Phys. 35 (2002) R1.
[10] K. Kawase, M. Sato, K. Nakamura, T. Taniuchi, H. Ito, Appl. Phys. Lett. 71 (1996) 753.
[11] A. Hamster, PhD thesis, University of Twente (1999) 35.